

Joint Route Optimization and Multi-Dimensional Resource Management Scheme for Airborne Radar Network in Target Tracking Application

Chenguang Shi, *Member, IEEE*, Xiangrong Dai, Yijie Wang, Jianjiang Zhou, *Member, IEEE*, and Sana Salous, *Senior Member, IEEE*

Abstract—In this paper, we investigate the problem of joint route optimization and multi-dimensional resource management for airborne radar network in target tracking application. The mechanism of the proposed joint route optimization and multi-dimensional resource management (JRO-MDRM) scheme is to adopt the optimization technique to collaboratively design the flight route, transmit power, dwell time, waveform bandwidth, and pulse length of each airborne radar node subject to the system kinematic limitations and several resource budgets, with the aim of simultaneously enhancing the target tracking accuracy and low probability of intercept (LPI) performance of the overall system. The predicted Bayesian Cramér-Rao lower bound (BCRLB) and probability of intercept are calculated and employed as the metrics to gauge the target tracking performance and LPI performance, respectively. It is shown that the resulting optimization problem is non-linear and non-convex, and the corresponding working parameters are coupled in both objective functions, which is generally intractable. By incorporating the particle swarm optimization (PSO) and cyclic minimization approaches, an efficient four-step solution algorithm is proposed to deal with the above problem. Extensive numerical results are provided to demonstrate the correctness and advantages of our developed scheme compared with other existing benchmarks.

Index Terms—Joint route optimization and multi-dimensional resource management (JRO-MDRM), airborne radar network, target tracking, Bayesian Cramér-Rao lower bound (BCRLB), low probability of intercept (LPI), particle swarm optimization (PSO).

I. INTRODUCTION

A. Background and Literature Review

With the significant superiorities over the static radar systems, the airborne radar network has received considerable interests in various applications, such as air defence, missile guidance, cooperative navigation, target localization, and so

forth. By employing the high flexibility and mobility of airborne platforms, the system performance of the airborne radar network can remarkably be improved by adaptively and rapidly coordinating their flight routes and transmit resources according to different tasks [1]-[3]. In such a case, this kind of system is able to collect much more sufficient information with multiple airborne nodes from different areas of interest.

In reality, although the airborne radar network system enjoys great benefits, several technical problems need to be tackled to unlock the promised performance gains. On the one hand, since the flight route of airborne radar node can be adjusted based on the real-time battlefield situation, the route optimization has offered a promising idea to detect and track hostile targets. For example, in [4], Zhou et al. utilize the distance-only measurements to design the optimal motion strategies for mobile sensors in target tracking scenario, and two different algorithms are proposed to determine the set of feasible positions that each sensor node should move to at each time index. In [5], the authors investigate the problem of joint path planning and sensor subset selection for multistatic sensor network, and a genetic approach-based solution methodology is developed to obtain the suboptimal solutions to the above intractable problem. Also, the impacts of sensor location uncertainties due to deployment error and sensor drifting on the target tracking accuracy is analyzed. A communication-constrained motion path planning algorithm for networked robotic surveillance is presented in [6], which aims to minimize the probability of target detection error subject to the predefined requirements on the connectivity of the robots to the control center. Reference [7] proposes a unmanned aerial vehicle (UAV) path planning approach for emitter localization by employing several passive payload sensors. Ragi et al. in [8] build the problem of UAV path planning as a partially observable Markov decision process. The work in [9] addresses the problem of joint optimization of transmitter waveform and receiver path for target tracking in a multistatic radar system, whose purpose is to minimize the tracking error by taking advantages of both waveform-only and path-only optimization methods. In [10], a moving target detection scheme utilizing colocated multiple-input multiple-output (MIMO) radar on multiple distributed moving platforms is studied, and a compressed sensing-based model is established to further employ the clutter sparsity in the surveillance region. The study of [11] optimizes the UAV path for joint detection and tracking of multiple radio-tagged targets. Other existing works can refer to [12]-[14].

Manuscript revised August 1, 2021. This work is supported in part by the National Natural Science Foundation of China under Grant 61801212, in part by the Key Laboratory of Equipment Pre-Research Foundation under Grant 6142401200402, in part by the National Science Foundation of Jiangsu Province under Grant BK20180423, in part by the National Aerospace Science Foundation of China under Grant 20200020052002 and Grant 20200020052005, in part by National Defense Science and Technology Innovation Special Zones, and in part by Key Laboratory of Radar Imaging and Microwave Photonics (Nanjing Univ. Aeronaut. Astronaut.), Ministry of Education, Nanjing, China. (*Corresponding author: C. G. Shi.*)

C. G. Shi, X. R. Dai, Y. J. Wang, and J. J. Zhou are with Key Laboratory of Radar Imaging and Microwave Photonics (Nanjing University of Aeronautics and Astronautics), Ministry of Education, Nanjing University of Aeronautics and Astronautics, Nanjing 210016, China.

S. Salous is with School of Engineering and Computing Sciences, Durham University, Durham, DH1 3LE, U.K..

On the other hand, the transmit resource of an airborne radar is usually limited due to the weight and size restrictions of the airborne platform. Besides, the low probability of intercept (LPI) issue is a crucial and essential demand of military applications in modern battlefield [15]-[19]. As a consequence, the problem of resource-aware management in radar systems has drawn great research interests so far, which aims to achieve much better resource utilization efficiency. For instance, in [20], Yi et al. propose a joint beam and power scheduling algorithm for distributed multiple targets tracking in netted colocated MIMO radar architectures. It is shown that the tracking accuracies of multiple targets are significantly enhanced, and the communication requirements between different radar nodes are reduced while meeting the robustness of the overall system. The authors in [21] address the problem of joint target assignment and power allocation for multiple distributed MIMO radar networks in clutter, where the radar node works in a defocused transmit-focused receive manner. Furthermore, Zhang et al. develop an efficient power allocation technique for maneuvering target tracking in a cognitive colocated MIMO radar system [22], and the sequential relaxation-based solver is put forth to deal with the formulated optimization problem. The study in [23] concentrates on the target capacity-based resource optimization for multi-target tracking in radar network, which jointly designs the illumination power and dwell time of different radar nodes to maximize the number of the targets that can be tracked with specified accuracy demands. By exploiting relaxation and tuning process, the original non-smooth optimization model is solved. It is worth to mention that not only transmit resources but also waveform parameters have effects on the target tracking performance. Thus, Cheng et al. in [24] formulate the optimization model for joint time-space resource allocation and waveform selection for colocated MIMO radar in multi-target tracking, where the objective function in terms of system resource consumption and target tracking accuracy is minimized by adaptively coordinating the **variables of interest**, i.e., revisit interval, sub-array number, transmit energy, and waveform parameters. More recently, reference [25] extends the work of [24] to netted colocated MIMO radar case in order to achieve better trade-off between illumination resource burden and target tracking precision.

In light of the aforementioned references, although there have been vast studies on flight route optimization and resource scheduling on demand, the above two aspects are always considered separately. The authors in [2] propose a joint online route planning and power allocation strategy for multi-target tracking in a monostatic airborne radar, whereas only the heading angle and transmit power are optimized, whose application is very limited. In addition, as stated previously, even though the transmit waveform selection and receiver path are jointly selected by a multistatic radar system in [9], the kinematic velocity, transmit power and dwell time of each airborne node are ignored. Therefore, it is interesting and meaningful to integrate the route planning and transmit resource management frameworks into a coherent one to offer more freedom for system performance gains. Nevertheless, the joint optimization of route planning and multi-dimensional resource management for airborne radar network in target

tracking environment is very challenging and remains to be investigated. This gap motivates this work.

B. Our Contributions

In the current work, we put forward a joint route optimization and multi-dimensional resource management (JRO-MDRM) scheme for airborne radar network system in target tracking scenario. Particularly, the adaptable working parameters in terms of flight route, transmit power, dwell time, waveform bandwidth, and pulse length of each airborne node are collaboratively designed to minimize the target tracking error and probability of intercept meanwhile for several system constraints. Also, an iterative and efficient four-step solution method is developed to solve the resulting non-linear and non-convex optimization problem. In short, we concentrate on how to optimize the flight route and multi-dimensional transmit resources for the purpose of target tracking accuracy and LPI performance improvements.

Our contributions of this paper are summed up as follows:

- 1) The problem of JRO-MDRM for airborne radar network in target tracking application is formulated as a mathematical optimization model under the constraints of system kinematic limitations and transmit resource budgets. In general, the JRO-MDRM scheme is a mathematical problem of simultaneously optimizing the target tracking accuracy and LPI performance of the underlying system while meeting certain system constraints. Here, the analytical expressions for the predicted BCRLB and the probability of intercept are derived and then employed to evaluate the target tracking accuracy and LPI performance of the airborne radar network, respectively. It is also noted that both criterion functions are related to the corresponding working variables. More specifically, the key idea of the JRO-MDRM scheme is to minimize the predicted BCRLB for target tracking and the probability of intercept in the meantime by jointly coordinating the flight route, transmit power, dwell time, waveform bandwidth, and pulse length of each airborne node while guaranteeing the given constraint conditions.
- 2) Since the formulated optimization model is non-linear and non-convex, and the closed-form expressions for the criterion functions are complex, it is generally intractable and cannot be tackled directly by exploiting the existing optimization techniques. To this end, we develop an iterative and efficient four-step solution algorithm incorporating particle swarm optimization (PSO) and cyclic minimization approaches to acquire the suboptimal solutions to the resulting problem. Numerical results are provided to validate the effectiveness and superiority of the developed JRO-MDRM scheme compared with other state-of-the-art baseline algorithms.

The remainder of this paper is organized as follows: In **Section II**, we describe the related system model. In **Section III**, we present the optimization problem formulation for JRO-MDRM in airborne radar network. **Section IV** proposes an efficient iteration method to solve the formulated optimization problem. **Section V** provides several numerical simulations

to demonstrate that the performance of the proposed JRO-MDRM scheme outperforms other existing benchmarks. Finally, Section VI concludes this paper. The related notations are explained when they are first exploited.

Notations: The superscript $(\cdot)^T$ denotes the transpose operator, \otimes denotes the Kronecker product operator.

II. SYSTEM MODEL

Consider an airborne radar network, which is composed of N widely separated airborne radars moving in a Cartesian coordinate and guaranteeing synchronized time. The position of the n -th radar node at each tracking interval k is represented by $[x_{n,k}, y_{n,k}]$. To facilitate the system design and simplicity, each airborne radar works in a monostatic manner and can only process the target echoes due to its own emitted signals. Note that the working parameters of each airborne radar node are the route planning, transmit power, dwell time, waveform bandwidth, and pulse length. The goal of the airborne radar network is to track the single target and obtain the estimates of target range, Doppler shift, and angle of arrival.

To start with, the following moderate assumptions are made to simplify the problem: (1) The emitted signal of each airborne radar node is a narrow-band signal. (2) The n -th airborne node is equipped with only a matched filter that correlates to its own transmitted waveform. (3) The time compression due to the Doppler shift is ignored. (4) The passive interceptor is carried on the moving target with an omni-directional receiving antenna. (5) The target track can be initialized by exploiting the multi-frame detection or Hough transform techniques.

A. Target Dynamic Model

The target state at frame k is $\mathbf{x}_k = [x_k, y_k, \dot{x}_k, \dot{y}_k]^T$, where $[x_k, y_k]$ denotes the target position at the k -th time slot, and $[\dot{x}_k, \dot{y}_k]$ denotes the target velocity at the k -th time slot. It is also supposed that the target track has been initialized by employing different algorithms [26]. Then, the target dynamic model can be given by:

$$\mathbf{x}_k = \mathbf{F}\mathbf{x}_{k-1} + \mathbf{w}_{k-1}, \quad (1)$$

where \mathbf{F} stands for the target state transition matrix. In this paper, the target motion is described by the following two models, that is, one constant-velocity (CV) model and one coordinated turning (CT) models with different rotation factors. To be specific, the target state transition matrix for the CV model \mathbf{F}_{CV} is expressed by:

$$\mathbf{F}_{CV} = \begin{bmatrix} 1 & 0 & \Delta T & 0 \\ 0 & 1 & 0 & \Delta T \\ 0 & 0 & 1 & 0 \\ 0 & 0 & 0 & 1 \end{bmatrix}, \quad (2)$$

where ΔT denotes the revisit interval between two successive tracking frames. Also, the target state transition matrix for the CT model \mathbf{F}_{CT} can be written as:

$$\mathbf{F}_{CT} = \begin{bmatrix} 1 & \frac{\sin(\omega\Delta T)}{\omega} & 0 & \frac{\cos(\omega\Delta T)-1}{\omega^2} \\ 0 & \cos(\omega\Delta T) & 0 & -\frac{\sin(\omega\Delta T)}{\omega} \\ 0 & \frac{1-\cos(\omega\Delta T)}{\omega} & 1 & \frac{\sin(\omega\Delta T)}{\omega} \\ 0 & \sin(\omega\Delta T) & 0 & \cos(\omega\Delta T) \end{bmatrix}, \quad (3)$$

where ω is the angular speed of turning. The term \mathbf{w}_{k-1} in Equation (2) denotes the zero-mean Gaussian process noise with a known covariance matrix \mathbf{Q}_{k-1} as:

$$\mathbf{Q}_{k-1} = \begin{bmatrix} \frac{(\Delta T)^3}{3} & \frac{(\Delta T)^2}{2} \\ \frac{(\Delta T)^2}{2} & \Delta T \end{bmatrix} \otimes (\gamma\mathbf{I}_2), \quad (4)$$

where γ denotes the intensity level of process noise.

B. Airborne Radar Dynamic Model

It is indicated in [2][9] that the motion of each airborne radar node can also be built as a discrete time kinematic model, which consists of its location, kinematic velocity, and heading angle. Thus, the dynamic model of the n -th airborne radar node is expressed by:

$$\begin{cases} x_{n,k} = x_{n,k-1} + \frac{v_{n,k}\cos\phi_{n,k} + v_{n,k-1}\cos\phi_{n,k-1}}{2} \Delta T, \\ y_{n,k} = y_{n,k-1} + \frac{v_{n,k}\sin\phi_{n,k} + v_{n,k-1}\sin\phi_{n,k-1}}{2} \Delta T, \end{cases} \quad (5)$$

where $v_{n,k}$ and $\phi_{n,k}$ represent its kinematic velocity and heading angle, respectively.

C. Measurement Model

The measurements \mathbf{z}_k from different airborne radar nodes at frame k have the form $\mathbf{z}_k = [\mathbf{z}_{1,k}^T, \dots, \mathbf{z}_{n,k}^T, \dots, \mathbf{z}_{N,k}^T]^T$, where the measurement acquired by the n -th airborne node $\mathbf{z}_{N,k}$ can be expressed by [26][27]:

$$\mathbf{z}_{n,k} = \mathbf{h}_{n,k}(\mathbf{x}_k) + \mathbf{u}_{n,k}, \quad (6)$$

where $\mathbf{h}_{n,k}(\mathbf{x}_k)$ denotes the non-linear measurement function:

$$\mathbf{h}_{n,k}(\mathbf{x}_k) = \begin{bmatrix} R_{n,k} \\ v_{n,k} \\ \theta_{n,k} \end{bmatrix} = \begin{bmatrix} \sqrt{(x_k - x_n)^2 + (y_k - y_n)^2} \\ \frac{\dot{x}_k(x_k - x_n) + \dot{y}_k(y_k - y_n)}{\sqrt{(x_k - x_n)^2 + (y_k - y_n)^2}} \\ \arctan\left(\frac{y_k - y_n}{x_k - x_n}\right) \end{bmatrix}, \quad (7)$$

where $R_{n,k}$, $v_{n,k}$, and $\theta_{n,k}$ stand for the range, velocity, and angle of arrival measurement components at the n -th node, respectively. $\mathbf{h}(\mathbf{x}_k)$ represents the measurement function, $\mathbf{N}_{n,k}$ represents the measurement error matrix at frame k with covariance $\mathbf{\Psi}_{n,k}$. Thus, the dimension of the measurement is three, with

$$\begin{cases} R_{n,k} = \sqrt{(x_k - x_n)^2 + (y_k - y_n)^2}, \\ v_{n,k} = \frac{\dot{x}_k(x_k - x_n) + \dot{y}_k(y_k - y_n)}{\sqrt{(x_k - x_n)^2 + (y_k - y_n)^2}}, \\ \theta_{n,k} = \arctan\left(\frac{y_k - y_n}{x_k - x_n}\right). \end{cases} \quad (8)$$

It is worth mentioning that each airborne radar transmits the linear frequency modulation (LFM) signal with a complex Gaussian envelope. Thus, the measurement error covariance $\mathbf{\Psi}_{n,k}$ can be characterized by the waveform parameters, which is computed by [27]:

$$\mathbf{\Psi}_{n,k} = \mathbf{T}\mathbf{C}_{n,k}\mathbf{T}^T, \quad (9)$$

where $\mathbf{T} = \text{diag}[c/2, c/(2f_c), 1]$ is the transform matrix from time and Doppler shift to range and range rate, c is the speed of light, $\mathbf{C}_{n,k}$ is the Cramér-Rao lower bound (CRLB) matrix for

the radar estimates at node n . For the Gaussian-LFM signal, $\mathbf{C}_{n,k}$ can further be written as:

$$\mathbf{C}_{n,k} = \frac{1}{\text{SNR}_{n,k}} \begin{bmatrix} 2\lambda_{n,k}^2 & -4b_k\lambda_{n,k}^2 & 0 \\ -4b_k\lambda_{n,k}^2 & \frac{1}{2\pi^2\lambda_{n,k}^2} + 8b^2\lambda_{n,k}^2 & 0 \\ 0 & 0 & \sigma_\theta^2 \end{bmatrix}, \quad (10)$$

where $b_{n,k}$ represents the frequency modulation rate of radar n at frame k , $b_{n,k} = W_{n,k}/2T_{s,n,k}$, $W_{n,k}$ represents the bandwidth of the transmit waveform at frame k , $T_{s,n,k}$ denotes the effective pulse length, $\lambda_{n,k}$ denotes the Gaussian pulse length parameter, and σ_θ^2 denotes the CRLB of the angle of arrival estimate. Note that the effective pulse length $T_{s,n,k}$ is approximately equal to $7.4338\lambda_{n,k}$, i.e., $T_{s,n,k} = 7.4338\lambda_{n,k}$ [27]. The term $\text{SNR}_{n,k}$ stands for the achieved signal to noise ratio of the n -th radar at frame k , which can be given by:

$$\text{SNR}_{n,k} = \frac{P_{t,n,k}T_{d,n,k}G_{t,n}G_{r,n}\sigma_n\lambda_t^2G_{RP}}{(4\pi)^3T_rR_{n,k}^4k_0T_0B_rF_r}, \quad (11)$$

where $P_{t,n,k}$ is the transmit power of radar n at time slot k , $T_{d,n,k}$ is the corresponding dwell time, σ_n is the RCS of target with respect to radar n , $G_{t,n}$ is the gain of transmitting antenna at the n -th radar node, $G_{r,n}$ is the gain of receiving antenna at the n -th radar, G_{RP} is the processing gain of each radar, T_r is the pulse repetition rate, F_r denotes the noise coefficient of each radar receiver, k_0 denotes Boltzmann constant, T_0 denotes the noise temperature of each radar receiver, B_r denotes the bandwidth of each radar receiver, λ_t denotes the signal wavelength, and $R_{n,k}$ represents the range from the target to the n -th airborne node at time slot k .

III. PROPOSED JRO-MDRM SCHEME FOR AIRBORNE RADAR NETWORK

A. Basis of the Technique

Mathematically, the proposed JRO-MDRM scheme can be regarded as an optimization problem of simultaneously improving the target tracking accuracy and LPI performance of the airborne radar network under the constraints of kinematic limitations and certain system resource budgets. The predicted BCRLB and probability of intercept are derived and adopted as the metrics to evaluate the target tracking performance and LPI performance, respectively. The adaptable variables considered here are the kinematic velocity $v_{n,k}$, heading angle $\phi_{n,k}$, transmit power $P_{t,n,k}$, dwell time $T_{d,n,k}$, waveform bandwidth $W_{n,k}$, and pulse length $\lambda_{n,k}$ of the n -th airborne node at the k -th tracking instant. For the sake of convenience, we collect the working parameters of the overall system as \mathbf{v}_k , ϕ_k , $\mathbf{P}_{t,k}$, $\mathbf{T}_{d,k}$, \mathbf{W}_k , and $\boldsymbol{\lambda}_k$, to represent the working parameters corresponding to all the airborne nodes, that is:

$$\begin{cases} \mathbf{v}_k = [v_{1,k}, \dots, v_{N,k}]^T, \phi_k = [\phi_{1,k}, \dots, \phi_{N,k}]^T, \\ \mathbf{P}_{t,k} = [P_{t,1,k}, \dots, P_{t,N,k}]^T, \mathbf{T}_{d,k} = [T_{d,1,k}, \dots, T_{d,N,k}]^T, \\ \mathbf{W}_k = [W_{1,k}, \dots, W_{N,k}]^T, \boldsymbol{\lambda}_k = [\lambda_{1,k}, \dots, \lambda_{N,k}]^T. \end{cases} \quad (12)$$

We are then in a position to optimize the above parameters in order to achieve better target tracking accuracy and LPI performance for the airborne radar network system. The detailed steps of the JRO-MDRM scheme are given in the following.

B. The Predicted BCRLB

It is well-known that the BCRLB is able to bound the error variance of the target state estimation, and it is predictive at one step ahead in the tracking recursion cycle. Intuitively, the predicted BCRLB is employed here as a performance metric to gauge the target tracking accuracy for our proposed JRO-MDRM algorithm. Additionally, we assume that the measurements obtained from multiple airborne radar nodes are independent with each other [19]-[23]. Therefore, the predicted Bayesian information matrix (BIM) is written as:

$$\begin{aligned} & \mathbf{J}(\mathbf{x}_{k|k-1}, \mathbf{v}_k, \phi_k, \mathbf{P}_{t,k}, \mathbf{T}_{d,k}, \mathbf{W}_k, \boldsymbol{\lambda}_k) \\ &= \mathbf{J}_P(\mathbf{x}_{k-1}, \mathbf{v}_{k-1}, \phi_{k-1}, \mathbf{P}_{t,k-1}, \mathbf{T}_{d,k-1}, \mathbf{W}_{k-1}, \boldsymbol{\lambda}_{k-1}) \\ &+ \mathbf{J}_Z(\mathbf{x}_{k|k-1}, \mathbf{v}_k, \phi_k, \mathbf{P}_{t,k}, \mathbf{T}_{d,k}, \mathbf{W}_k, \boldsymbol{\lambda}_k), \end{aligned} \quad (13)$$

where $\mathbf{x}_{k|k-1}$ represents the predicted target state vector at the $(k-1)$ -th time slot, $\mathbf{J}_P(\mathbf{x}_{k-1}, \mathbf{v}_{k-1}, \phi_{k-1}, \mathbf{P}_{t,k-1}, \mathbf{T}_{d,k-1}, \mathbf{W}_{k-1}, \boldsymbol{\lambda}_{k-1})$ represents the prior information BIM, and $\mathbf{J}_Z(\mathbf{x}_{k|k-1}, \mathbf{v}_k, \phi_k, \mathbf{P}_{t,k}, \mathbf{T}_{d,k}, \mathbf{W}_k, \boldsymbol{\lambda}_k)$ represents the measurement BIM. Based on the derivations in previous references, the closed-form expression for the predicted BIM can be given at the top of the next page, where $\mu_{m,k|k-1}$ denotes the predicted probability of model m at the $(k-1)$ -th time slot, \mathbf{F}_m denotes the state transition matrix of model m with $\mathbf{F}_m \in \{\mathbf{F}_{CV}, \mathbf{F}_{CT}\}$, and $\mathbf{H}_{n,k} = [\nabla_{\mathbf{x}_{k|k-1}} (\mathbf{h}_{n,k}(\mathbf{x}_{k|k-1}))^T]^T$ denotes the Jacobian matrix of the non-linear measurement function.

In the end, since the predicted BCRLB is the inverse of the predicted BIM, it can be expressed by:

$$\mathbf{C}_{\text{BCRLB},k} = [\mathbf{J}(\mathbf{x}_{k|k-1}, \mathbf{v}_k, \phi_k, \mathbf{P}_{t,k}, \mathbf{T}_{d,k}, \mathbf{W}_k, \boldsymbol{\lambda}_k)]^{-1}, \quad (15)$$

where the diagonal elements of the matrix $\mathbf{C}_{\text{BCRLB},k}$ denote the lower bounds on the variances of the predicted estimates of target motion state, respectively.

C. The Probability of Intercept

It is known that there are several metrics that can be adopted to evaluate the LPI performance of different radar systems, such as Schleher intercept factor, probability of intercept, radio frequency intensity, etc. In the current study, the probability of intercept is utilized to assess the LPI performance for the airborne radar network system. Technically speaking, the analytical expression for the probability of intercept can be viewed as a function of various variables, for instance, the illumination power, dwell time, revisit interval, search time of interceptor, and so on. Hence, the probability of intercept for the n -th airborne radar node at the k -th tracking instant can be expressed at the top of the next page, where T_I denotes the search time of intercept receiver, p_{fa} denotes the probability of false alarm of interceptor, $G_{t,n}$ denotes the transmitting antenna gain of radar n , G_I denotes the receiving antenna gain of the hostile passive intercept receiver, G_{IP} denotes the processing gain of interceptor, B_I denotes the frequency bandwidth of interceptor, F_I denotes the noise factor of interceptor, and $R_{n,k|k-1}$ denotes the predicted range between the airborne node and the target at the k -th time index.

$$\begin{aligned} & \mathbf{J}(\mathbf{x}_{k|k-1}, \mathbf{v}_k, \phi_k, \mathbf{P}_{t,k}, \mathbf{T}_{d,k}, \mathbf{W}_k, \lambda_k) \\ &= \sum_{m=1}^3 [\mu_{m,k|k-1} [\mathbf{Q}_{k-1} + \mathbf{F}_m \mathbf{J}(\mathbf{x}_{k-1}, \mathbf{v}_k, \phi_k, \mathbf{P}_{t,k}, \mathbf{T}_{d,k}, \mathbf{W}_k, \lambda_k) \mathbf{F}_m^T]^{-1}] + \sum_{n=1}^N \left[\mathbf{H}_{n,k}^T \boldsymbol{\Psi}_{n,k}^{-1} \mathbf{H}_{n,k} \right] \Big|_{\mathbf{x}_{k|k-1}} \end{aligned} \quad (14)$$

$$p_{I,n,k}(v_{n,k}, \phi_{n,k}, P_{t,n,k}, T_{d,n,k}) = \frac{T_{d,n,k}}{2T_1} \times \left[1 - \frac{2}{\sqrt{\pi}} \int_0^{\sqrt{-\ln p_{fa}'} - \sqrt{\frac{P_{t,n,k} G_{t,n} G_1 \lambda_k^2 G_{IP}}{(4\pi)^2 R_{n,k|k-1}^{k_0 T_0 B_1 F_1} + 0.5}}} \exp(-z^2) dz \right] \quad (16)$$

Due to the fact that there exists multiple active radars in the airborne radar network architecture, the overall probability of intercept at the k -th time index can be defined as follows to evaluate the LPI performance of the underlying system:

$$\begin{aligned} & p_{I,k}^{\text{tot}}(\mathbf{v}_k, \phi_k, \mathbf{P}_{t,k}, \mathbf{T}_{d,k}) \\ & \triangleq 1 - \prod_{n=1}^N [1 - p_{I,n,k}(v_{n,k}, \phi_{n,k}, P_{t,n,k}, T_{d,n,k})]. \end{aligned} \quad (17)$$

Remark 1: Without loss of generality, it is supposed that the corresponding parameters of the hostile passive intercept receiver, such as the search time, receiving antenna gain, processing gain, frequency bandwidth, etc, are known as prior information, which are available according to the military intelligence and knowledge.

Remark 2: According to above performance metrics in Equations (15) and (17), it is noticeable that the corresponding working parameters affect the proposed JRO-MDRM strategy. More specifically, not only the route planning but also the multi-dimensional resource has influence on the attainable target tracking accuracy and LPI performance.

D. Optimization Problem Formulation

In general, the primary goal of the proposed JRO-MDRM scheme is to minimize the achievable target tracking error and probability of intercept of the airborne radar network system in the meantime subject to the kinematic limitations and several resource budgets. By jointly designing the kinematic velocity, heading angle, transmit power, dwell time, waveform bandwidth, and pulse length of each airborne radar node, the optimization problem at each tracking frame k can be formulated in the following:

$$\begin{aligned} & \min_{\mathbf{v}_k, \phi_k, \mathbf{P}_{t,k}, \mathbf{T}_{d,k}, \mathbf{W}_k, \lambda_k} \mathbb{F}(\mathbf{v}_k, \phi_k, \mathbf{P}_{t,k}, \mathbf{T}_{d,k}, \mathbf{W}_k, \lambda_k), \\ & \min_{\mathbf{v}_k, \phi_k, \mathbf{P}_{t,k}, \mathbf{T}_{d,k}} p_{I,k}^{\text{tot}}(\mathbf{v}_k, \phi_k, \mathbf{P}_{t,k}, \mathbf{T}_{d,k}), \\ \text{s.t.:} & \begin{cases} C1: \bar{v}_{\min} \leq v_{n,k} \leq \bar{v}_{\max}, \forall n, \\ C2: |\phi_{n,k} - \phi_{n,k-1}| \leq \bar{\phi}_{\max}, \forall n, \\ C3: \bar{P}_{\min} \leq P_{t,n,k} \leq \bar{P}_{\max}, \forall n, \\ C4: T_r \leq T_{d,n,k} \leq \bar{T}_{\max}, \forall n, \\ C5: W_{n,k} \in W_{\text{set}}, \lambda_{n,k} \in \lambda_{\text{set}}, \forall n, \end{cases} \end{aligned} \quad (18)$$

where the criterion function for target tracking performance is defined as:

$$\begin{aligned} & \mathbb{F}(\mathbf{v}_k, \phi_k, \mathbf{P}_{t,k}, \mathbf{T}_{d,k}, \mathbf{W}_k, \lambda_k) \\ & \triangleq \sqrt{\mathbf{C}_{\text{BCRLB},k}(1,1) + \mathbf{C}_{\text{BCRLB},k}(3,3)}, \end{aligned} \quad (19)$$

\bar{v}_{\min} and \bar{v}_{\max} denote the minimum and maximum values of the kinematic velocity, $\bar{\phi}_{\max}$ denote the maximum turning angle, \bar{P}_{\min} and \bar{P}_{\max} denote the lower and upper bounds of the transmit power of each airborne radar node, T_r and \bar{T}_{\max} denote the minimum and maximum values of the dwell time of each airborne node, and W_{set} and λ_{set} denote the waveform bandwidth set and pulse length set respectively. $\mathbf{C}_{\text{BCRLB},k}(1,1)$ and $\mathbf{C}_{\text{BCRLB},k}(3,3)$ denote the first and third elements on the diagonal of the matrix $\mathbf{C}_{\text{BCRLB},k}$, respectively. The Constraint C2 implies the limitation of platform maneuverability, which means that the heading angle is constrained by $\phi_{n,k-1}$ and $\bar{\phi}_{\max}$. It should be noted that, as shown in Constraint C5, the waveform bandwidth $W_{n,k}$ and pulse length $\lambda_{n,k}$ can be properly selected from the pre-determined sets, that is, $W_{\text{set}} = \{W_{1,k}, W_{2,k}, \dots, W_{N_W,k}\}$, $\lambda_{\text{set}} = \{\lambda_{1,k}, \lambda_{2,k}, \dots, \lambda_{N_\lambda,k}\}$, where N_W and N_λ represent the corresponding cardinal numbers of those two sets. As such, the transmit waveform pair can be obtained in the library $\Omega \triangleq \{(W_{1,k}, \lambda_{1,k}), (W_{2,k}, \lambda_{1,k}), \dots, (W_{N_W,k}, \lambda_{N_\lambda,k})\}$.

Remark 3: For multiple targets tracking application, the proposed JRO-MDRM scheme is able to be transformed to several sub-problems of single target tracking by introducing new criteria functions, such as the scaled accuracy-based objective function in [20][28]. In this scenario, the resulting sub-problems can be resolved independently by the iterative four-step solution technique. Therefore, it should be pointed out that the JRO-MDRM algorithm can directly be extended to the multi-target tracking case, which will be investigated in the potential future work.

IV. PROBLEM SOLUTION

It has been mentioned before that the formulated optimization problem in (18) involves six adaptable parameters, that is, kinematic velocity \mathbf{v}_k , heading angle ϕ_k , transmit power $\mathbf{P}_{t,k}$, dwell time $\mathbf{T}_{d,k}$, waveform bandwidth \mathbf{W}_k , and pulse length λ_k . One can notice that the developed JRO-MDRM scheme is a non-linear and non-convex optimization model, and the corresponding variables are coupled in both criterion

functions, which are generally intractable and cannot be dealt with directly by using the existing optimization methods [29]. In such a case, an iterative and efficient four-step solution approach, which incorporates PSO and cyclic minimization techniques, is proposed to obtain the suboptimal solutions to the above problem.

A. Four-Step Solution Technique

1) Problem Reformulation:

By introducing two weights w_1 and w_2 for the two criterion functions, the bi-objective optimization problem in (18) can be reformulated as:

$$\begin{aligned} \min_{\mathbf{v}_k, \phi_k, \mathbf{P}_{t,k}, \mathbf{T}_{d,k}, \mathbf{W}_k, \lambda_k} & w_1 \cdot \mathbb{F}(\mathbf{v}_k, \phi_k, \mathbf{P}_{t,k}, \mathbf{T}_{d,k}, \mathbf{W}_k, \lambda_k) \\ & + w_2 \cdot p_{1,k}^{\text{tot}}(\mathbf{v}_k, \phi_k, \mathbf{P}_{t,k}, \mathbf{T}_{d,k}), \\ \text{s.t.:} & \text{C1} - \text{C5}. \end{aligned} \quad (20)$$

where w_1 and w_2 represent the weights for target tracking accuracy and LPI performance, respectively. The parameters w_1 and w_2 are set based on different preferences for target tracking and LPI performance, respectively. If the target tracking performance is preferred, the weight w_1 can be set as a larger value, and vice versa.

On the other side, since the multiple airborne nodes work independently of each other, the optimization model in (20) can equivalently be converted to the following form:

$$\begin{aligned} \min_{\mathbf{v}_k, \phi_k, \mathbf{P}_{t,k}, \mathbf{T}_{d,k}, \mathbf{W}_k, \lambda_k} & w_1 \cdot \mathbb{F}(\mathbf{v}_k, \phi_k, \mathbf{P}_{t,k}, \mathbf{T}_{d,k}, \mathbf{W}_k, \lambda_k) \\ & + w_2 \cdot p_{1,n,k}(v_{n,k}, \phi_{n,k}, P_{t,n,k}, T_{d,n,k}), \\ \text{s.t.:} & \text{C1} - \text{C5}. \end{aligned} \quad (21)$$

2) Flight Route Optimization:

According to [2][9][19][25], in order to solve the NP-hard problem, an intuitive and reasonable solution is to partition the route optimization and illumination resource scheduling. Thus, for the predefined transmit parameters, i.e., $\mathbf{v}_k = \hat{\mathbf{v}}_k$, $\phi_k = \hat{\phi}_k$, $\mathbf{P}_{t,k} = \hat{\mathbf{P}}_{t,k}$, $\mathbf{T}_{d,k} = \hat{\mathbf{T}}_{d,k}$, $\mathbf{W}_k = \hat{\mathbf{W}}_k$, and $\lambda_k = \hat{\lambda}_k$, the optimization problem in (21) can further be given by:

$$\begin{aligned} \min_{\mathbf{v}_k, \phi_k} & w_1 \cdot \mathbb{F}(\mathbf{v}_k, \phi_k, \hat{\mathbf{P}}_{t,k}, \hat{\mathbf{T}}_{d,k}, \hat{\mathbf{W}}_k, \hat{\lambda}_k) \\ & + w_2 \cdot p_{1,n,k}(v_{n,k}, \phi_{n,k}, \hat{P}_{t,n,k}, \hat{T}_{d,n,k}), \\ \text{s.t.:} & \text{C1}, \text{C2}. \end{aligned} \quad (22)$$

It is widely known that the brute force search method or the exhaustive search technique can be utilized to solve the optimization model in (22). However, the above two algorithms need an exponential computational complexity. In the current work, we turn to the means of PSO for solving the problem of route optimization. It is well-known that the PSO technique has been widely used in engineering practice due to its quick convergence and easy implementation [30]. During the iteration procedure, each particle, which represents a single solution, adjusts its own position and velocity according to its best previous search experience and the best experience of

other neighbors. The velocity and position of the q -th particle can be updated as follows:

$$\begin{cases} \mathbf{V}_q^{(l+1)} = \zeta \mathbf{V}_q^{(l)} + c_1 r_1 (\mathbf{P}_q^{(l)} - \mathbf{Y}_q^{(l)}) \\ \quad + c_2 r_2 (\mathbf{P}_g^{(l)} - \mathbf{Y}_q^{(l)}), \\ \mathbf{Y}_q^{(l+1)} = \mathbf{Y}_q^{(l)} + \mathbf{V}_q^{(l+1)}, \end{cases} \quad (23)$$

where $\mathbf{V}_q^{(l+1)}$ and $\mathbf{Y}_q^{(l+1)}$ represent the velocity and position of the q -th particle at iteration l , respectively. ζ represents the inertia weight, and c_1 and c_2 represent two non-negative constants, which are referred to as acceleration factors. r_1 and r_2 represent the uniformly distributed random numbers between 0 and 1, and l represents the iteration index. $\mathbf{P}_q^{(l)}$ denotes the best solution that the q -th particle has achieved until the l -th iteration, and $\mathbf{P}_g^{(l)}$ denotes the best solution acquired in the whole population at the l -th iteration.

In problem (22), our main objective is to minimize the target tracking error and probability of intercept at the same time by adaptively optimizing the kinematic velocity and heading angle of each airborne node. Intuitively, these motion parameters are mapped to the positions of the particles. Then, the criterion function shown in (22) is employed as the fitness function $f(\mathbf{Y}_q^{(l)})$ for the problem of flight route optimization. In the end, all the particles are able to converge to the global optimal points through iterative computation and interaction with each other [30]. The detailed steps are summarized in Algorithm 1, according to which we can obtain the best flight route subject to the given kinematic limitations.

Algorithm 1: The General Steps of the PSO Algorithm for Flight Route Optimization

Input: Initialize Q particles with position $\mathbf{Y}_q^{(0)}$ and velocity $\mathbf{V}_q^{(0)}$ satisfying the constraint in (22), the inertia weight ζ , the acceleration factors c_1 and c_2 , the random numbers r_1 and r_2 , the iteration index l , and the maximum iteration number L_{\max} .

Output: The global optimal solutions.

```

1 repeat
2   Calculate the fitness function for  $\mathbf{Y}_q^{(l)}$ ;
3   if  $f(\mathbf{Y}_q^{(l)}) < P_q^{(l)}$  then
4     |  $P_q^{(l)} \leftarrow \mathbf{Y}_q^{(l)}$ ;
5   end
6   if  $f(\mathbf{Y}_q^{(l)}) < P_g^{(l)}$  then
7     |  $P_g^{(l)} \leftarrow \mathbf{Y}_q^{(l)}$ ;
8   end
9   Update the velocity and position of each particle by
   using Equation (23);
10 until  $l > L_{\max}$  or convergence;
11 Output the final solutions.
```

2) Multi-Dimensional Transmit Resource Management:

After the feasible kinematic velocity and heading angle results of each airborne node, that is, $\hat{v}_{n,k}$ and $\hat{\phi}_{n,k}$, are obtained, the relevant variables can be removed from the

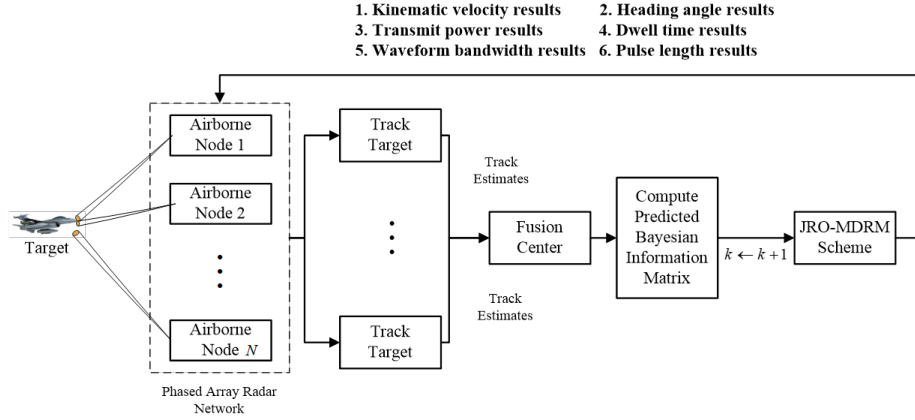


Fig. 1. The sketch map of the JRO-MDRM scheme.

optimization problem (21). Subsequently, we get the following problem as:

$$\begin{aligned}
 & \min_{\hat{\mathbf{v}}_k, \hat{\phi}_k, \mathbf{P}_{t,k}, \mathbf{T}_{d,k}, \mathbf{W}_k, \boldsymbol{\lambda}_k} w_1 \cdot \mathbb{F}(\hat{\mathbf{v}}_k, \hat{\phi}_k, \mathbf{P}_{t,k}, \mathbf{T}_{d,k}, \mathbf{W}_k, \boldsymbol{\lambda}_k) \\
 & + w_2 \cdot p_{l,n,k}(\hat{v}_{n,k}, \hat{\phi}_{n,k}, P_{t,n,k}, T_{d,n,k}), \\
 & \text{s.t.: } C3 - C5.
 \end{aligned} \tag{24}$$

Similar to the optimization problem in (22), the PSO algorithm can also be adopted to tackle the problem of multi-dimensional resource management in (24), where the difference is that the illumination power, dwell time, waveform bandwidth, and pulse length of each airborne radar are mapped to the positions of the particles.

4) *Cyclic Iteration*: Record the route optimization and multi-dimensional resource management results and the corresponding value of the criterion functions at each iterative step. Subsequently, *Step 2*) and *Step 3*) are calculated repeatedly, and the iteration stops when the difference in the obtained value of objective function between one iteration and another is much smaller than a given value. Ultimately, record the smaller value of the criterion function in (21) as the final result, while the corresponding flight route and transmit resource results are regarded as the final optimization results.

B. Closed-Loop Framework for the JRO-MDRM Scheme

In conclusion, the developed JRO-MDRM strategy exploits the feedback information in the target tracking cycle to perform the joint optimization in airborne radar network system. In this scenario, owing to the non-linearity of the measurement model, we utilize the interacting multiple model-extended Kalman filtering (IMM-EKF) approach to acquire the accurate target state estimate at each tracking frame. Then, the predicted BCRLB for target tracking is adopted to implement the JRO-MDRM algorithm. Finally, the flight route optimization and multi-dimensional transmit resource management results are sent back to design the probing strategy at the next frame, accomplishing the enhancements of target tracking accuracy and LPI performance in the meantime. The sketch map of the JRO-MDRM strategy for airborne radar network in target tracking is illustrated in Fig. 1.

TABLE I
SIMULATION PARAMETERS

Symbol	Value	Symbol	Value
$G_{t,n}(\forall n)$	36 dB	$G_{r,n}(\forall n)$	35 dB
G_I	10 dB	G_{IP}	3 dB
B_I	40 GHz	F_I	6 dB
G_{RP}	16.5 dB	F_r	3 dB
B_r	1 MHz	f_c	12 GHz
p'_{fa}	10^{-8}	ϕ_{\max}	15°
$\frac{v_{\min}}{v_{\max}}$	0.1 km/s	$\frac{v_{\max}}{v_{\min}}$	0.4 km/s
P_{\min}	0	P_{\max}	5 kW
T_r	5×10^{-4} s	T_{\max}	2.5×10^{-2} s

TABLE II
THE DESCRIPTION OF TARGET STATE

Time slots	Target motion
1 – 30s	Constant velocity
31 – 50s	Right turn($w = 3\text{rad}$)
51 – 80s	Constant velocity

V. NUMERICAL RESULTS

In this section, we demonstrate the performance of the proposed JRO-MDRM scheme via several numerical simulations. The airborne radar network system with $N = 4$ spatially diverse airborne radar nodes is taken into account. The waveform library Ω consists of 25 waveform types with $\lambda_{\text{set}} = [1, 3, 5, 7, 9]\mu\text{s}$ and $W_{\text{set}} = [0.1, 0.3, 0.5, 0.7, 0.9]\text{MHz}$. The revisit interval between two successive tracking frames is set to be $\Delta T = 1$ s, and the total number of tracking frames is $T_{\text{tot}} = 80$. The initial position and velocity of the target are set to be $[60, 80]$ km and $[150, 260]$ m/s, respectively. The search time of the hostile passive intercept receiver is $T_I = 2$ s. In the PSO method, we set $Q = 20$, $\zeta = 1$, $c_1 = 0.8$, $c_2 = 0.8$, and $L_{\max} = 50$. The other simulation parameters are summarized in TABLE I. In addition, the detailed description of the target state is given in TABLE II, while the initial states of multiple airborne radar nodes can be found in TABLE III.

TABLE III
THE DESCRIPTION OF AIRBORNE RADAR NETWORK

Index	Initial Position	Initial Velocity	Initial Heading Angle
1	[110, 0] km	0.4 km/s	0°
2	[50, -20] km	0.4 km/s	90°
3	[-20, 70] km	0.4 km/s	0°
4	[0, 150] km	0.4 km/s	90°

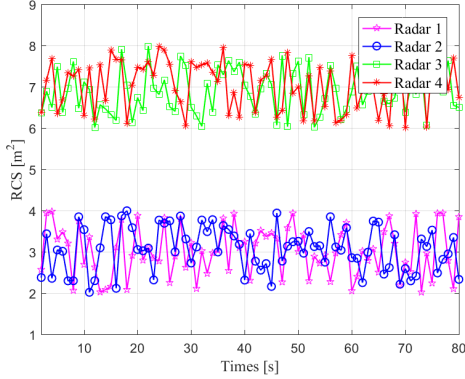


Fig. 2. The second target RCS model at each tracking frame.

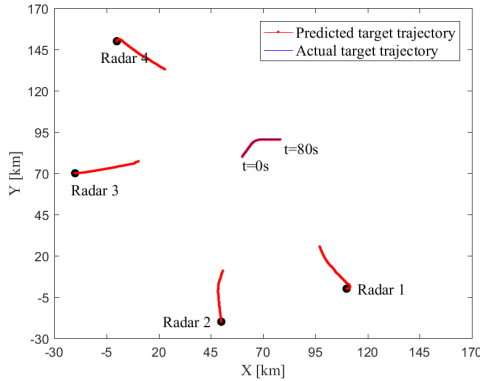


Fig. 3. The simulated tracking scenario in Experiment 1.

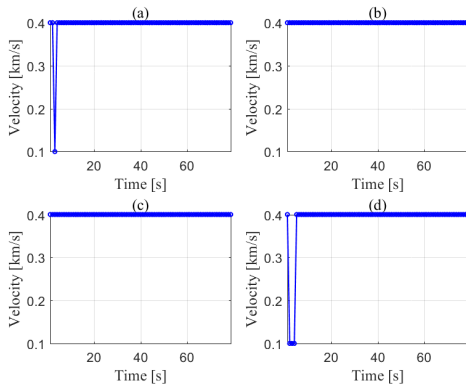


Fig. 4. Kinematic velocity optimization results of the JRO-MDRM scheme in Experiment 1: (a) Airborne radar node 1; (b) Airborne radar node 2; (c) Airborne radar node 3; (d) Airborne radar node 4.

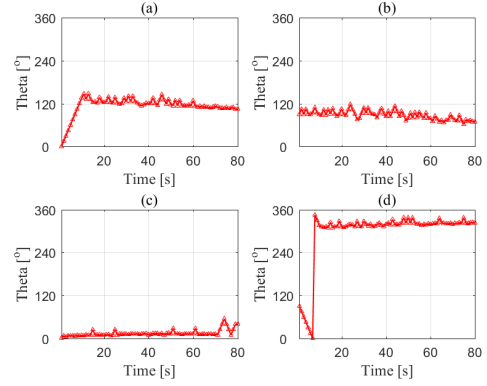


Fig. 5. Heading angle optimization results of the JRO-MDRM scheme in Experiment 1: (a) Airborne radar node 1; (b) Airborne radar node 2; (c) Airborne radar node 3; (d) Airborne radar node 4.

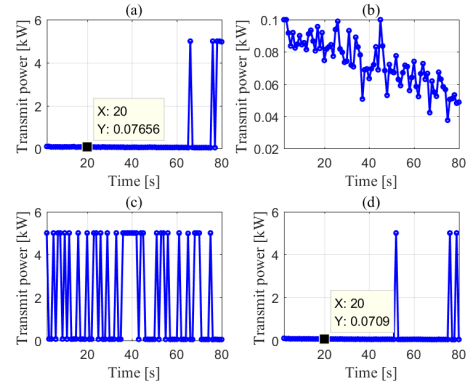


Fig. 6. Transmit power optimization results of the JRO-MDRM scheme in Experiment 1: (a) Airborne radar node 1; (b) Airborne radar node 2; (c) Airborne radar node 3; (d) Airborne radar node 4.

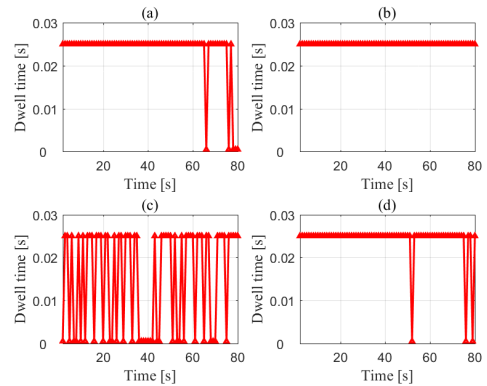


Fig. 7. Dwell time optimization results of the JRO-MDRM scheme in Experiment 1: (a) Airborne radar node 1; (b) Airborne radar node 2; (c) Airborne radar node 3; (d) Airborne radar node 4.

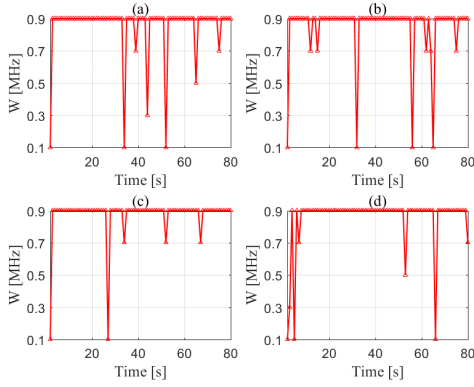


Fig. 8. Waveform bandwidth selection results of the JRO-MDRM scheme in Experiment 1: (a) Airborne radar node 1; (b) Airborne radar node 2; (c) Airborne radar node 3; (d) Airborne radar node 4.

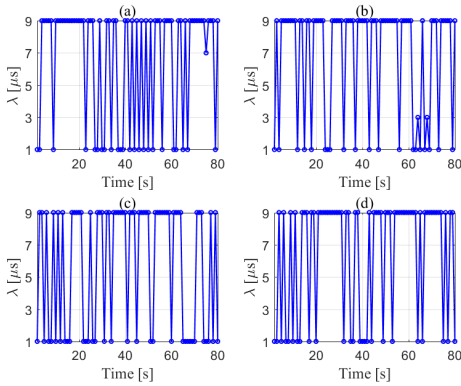


Fig. 9. Pulse length selection results of the JRO-MDRM scheme in Experiment 1: (a) Airborne radar node 1; (b) Airborne radar node 2; (c) Airborne radar node 3; (d) Airborne radar node 4.

A. Experiment 1: Target RCS Model 1

In this paper, in order to better examine the effect of the target reflectivity on the joint optimization results, we consider two different target radar cross section (RCS) models. In the first model, it is assumed that the target reflectivity is uniform and its RCS is set to be $\sigma_t = 3\text{m}^2$. While in the second one, the target reflectivities with respect to different airborne radar nodes are illustrated in Fig. 2, respectively. **It should be mentioned that the target reflectivity is assumed to obey normal distribution in the second RCS model, as depicted in Fig. 2, whereas our developed JRO-MDRM algorithm is applicable to different target RCS fluctuation models.**

Fig. 3 depicts the simulated target tracking scenario in Experiment 1, where the thick solid red lines show the optimized routes of multiple airborne radar nodes. The optimization results of kinematic velocity and heading angle of different airborne nodes are illustrated in Fig. 4 and Fig. 5, respectively. One can observe that the constraints of kinematic velocity and heading angle of each airborne node make the planned route smooth.

The transmit power and dwell time optimization results of the proposed JRO-MDRM scheme are respectively illustrated in Fig. 6 and Fig. 7, and the corresponding waveform

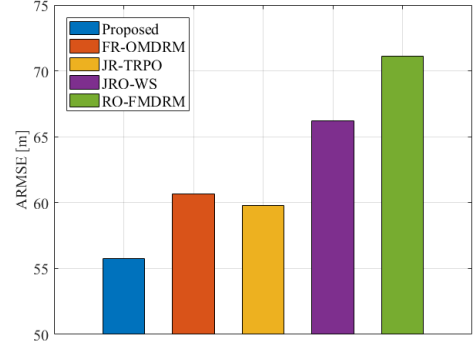


Fig. 10. Target tracking performance comparison in terms of the ARMSE by exploiting various approaches in Experiment 1.

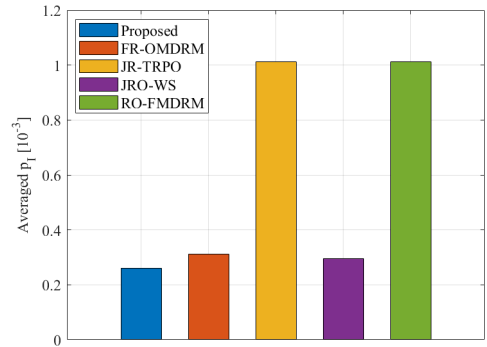


Fig. 11. LPI performance comparison in terms of the averaged probability of intercept by exploiting various approaches in Experiment 1.

bandwidth and pulse length selection results are shown in Fig. 8 and Fig. 9 respectively, which is obtained from a single Monte-Carlo simulation run. In Fig. 7, we can see that either the maximum value of dwell time or its minimum value is assigned to reduce the achievable probability of intercept of each airborne radar node, according to the target dynamic state in the tracking process. On the other hand, the illumination power of each airborne node is shown in Fig. 6, which is adaptively designed to minimize the metric for LPI performance of airborne radar network system.

Also, in Fig. 8 and Fig. 9, the waveform bandwidth and pulse length of each airborne radar node are adaptively chosen from the predefined parameter sets. As mentioned before, for each airborne node, there exists a relationship between transmit waveform parameters, that is, waveform bandwidth and pulse length, and target tracking BCRLB. Thus, combined with the obtained values of probing power and dwell time, the waveform bandwidth and pulse length are selected adaptively to optimize the target tracking accuracy by minimizing the criterion function in Equation (20), **which are the artifacts of the joint optimization.**

Moreover, in order to further disclose the advantages of the proposed JRO-MDRM scheme in terms of target tracking accuracy and LPI performance, its averaged root mean square

error (ARMSE) and the averaged probability of intercept are compared with those of the following four baseline methods in Fig. 10 and Fig. 11, respectively, which is conducted over 150 Monte-Carlo trials:

- Fixed route and optimal multi-dimensional resource management (FR-OMDRM): The multi-dimensional illumination resource management of each airborne radar node is implemented by solving the optimization model ($\mathbf{P0}$), whereas the corresponding kinematic velocity and heading angle are fixed to be their initial values, respectively.
- Joint route and transmit resource parameter optimization (JR-TRPO): The kinematic velocity, heading angle, transmit power, and dwell time of each airborne radar node are optimally designed by solving the optimization model ($\mathbf{P0}$), while the waveform bandwidth and pulse length are fixed to be 0.5MHz and $5\mu\text{s}$, respectively.
- Joint route optimization and waveform selection (JRO-WS): The kinematic velocity, heading angle, waveform bandwidth, and pulse length of each airborne radar node are jointly optimized by solving the optimization model ($\mathbf{P0}$), while the transmit power and dwell time are fixed to be 5kW and $5 \times 10^{-4}\text{s}$, respectively.
- Route optimization and fixed multi-dimensional resource management (RO-FMDRM): The route planning of each airborne node is optimized by adopting the PSO algorithm, whereas the multi-dimensional transmit resource parameters are set to be fixed, that is, the transmit power and dwell time are set to be 80W and $5 \times 10^{-4}\text{s}$ respectively, and the waveform parameters are set as $W = 0.5\text{MHz}$ and $\lambda = 5\mu\text{s}$ respectively.

The tracking ARMSE at each tracking frame k is defined at the top of the next page, where M_c denotes the total number of Monte-Carlo trials, and $[\hat{x}_{m,k|k}, \hat{y}_{m,k|k}]$ denotes the position estimate of the target at the m -th trial. The averaged probability of intercept of the airborne radar network can be calculated as:

$$\bar{p}_{1,k}^{\text{tot}}(\mathbf{v}_k, \phi_k, \mathbf{P}_{t,k}, \mathbf{T}_{d,k}) \triangleq \sum_{k=1}^{T_{\text{tot}}} p_{1,k}^{\text{tot}}(\mathbf{v}_k, \phi_k, \mathbf{P}_{t,k}, \mathbf{T}_{d,k}), \quad (63)$$

From the above figures, it is apparent that the JRO-MDRM algorithm exhibits the lowest values of ARMSE and averaged probability of intercept when compared with other baselines. The reason is that the proposed JRO-MDRM scheme is capable of collaboratively coordinating the kinematic velocity, heading angle, transmit power, dwell time, waveform bandwidth, and pulse length of each airborne radar node to minimize the dual-objective function in optimization problem ($\mathbf{P0}$). Therefore, it can be concluded that the JRO-MDRM scheme can not only reduce the target tracking error, but also enhance the LPI performance of airborne radar network, verifying its superiorities over other existing baselines.

B. Experiment 2: Target RCS Model 2

In this subsection, we expand the simulation to analyze the impact of the target reflectivity on the joint optimization results. For simplicity, it is supposed that the true RCS value of the target for the next time index is known as

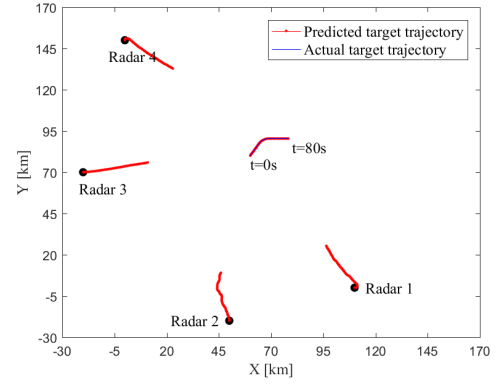


Fig. 12. The simulated tracking scenario in Experiment 2.

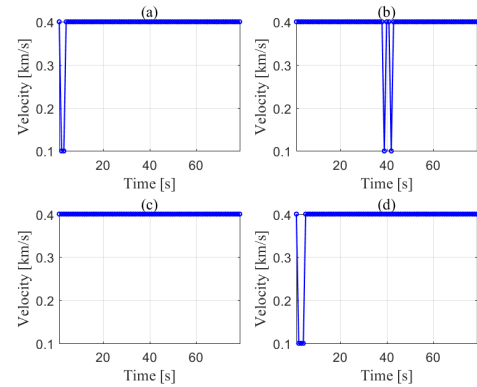


Fig. 13. Kinematic velocity optimization results of the JRO-MDRM scheme in Experiment 2: (a) Airborne radar node 1; (b) Airborne radar node 2; (c) Airborne radar node 3; (d) Airborne radar node 4.

prior knowledge to each airborne radar node. The simulated target tracking scenario in Experiment 2 is shown in Fig. 12, where the optimized kinematic velocity and heading angle of multiple airborne nodes are depicted in Fig. 13 and Fig. 14, respectively. Besides, the corresponding multi-dimensional illumination resource optimization results of each airborne radar node are given in Figures 15-18, which can help us have a deep understanding of the JRO-MDRM strategy. From the above figures, it is obvious that the change of target reflectivity will definitely have significant influence on the route planning and transmit resource management results of airborne radar network system.

Fig. 19 and Fig. 20 compare the achievable ARMSE and averaged probability of intercept of the proposed JRO-MDRM scheme with the other four baseline methods in Experiment 2, respectively. According to these two figures, it can be seen that our developed scheme is able to make better utilization of the available transmit resources of the overall system, and thus can acquire the best target tracking accuracy and LPI performance.

VI. CONCLUDING REMARKS

This paper put forwards a strategy to minimize the target tracking error and the probability of intercept of airborne

$$\text{ARMSE} \triangleq \sqrt{\frac{1}{M_{\text{tot}}} \sum_{k=1}^{M_{\text{tot}}} \frac{1}{M_c} \sum_{m=1}^{M_c} [(x_k - \hat{x}_{m,k|k})^2 + (y_k - \hat{y}_{m,k|k})^2]} \quad (62)$$

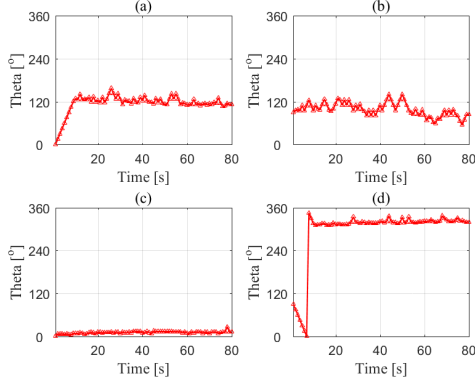


Fig. 14. Heading angle optimization results of the JRO-MDRM scheme in Experiment 2: (a) Airborne radar node 1; (b) Airborne radar node 2; (c) Airborne radar node 3; (d) Airborne radar node 4.

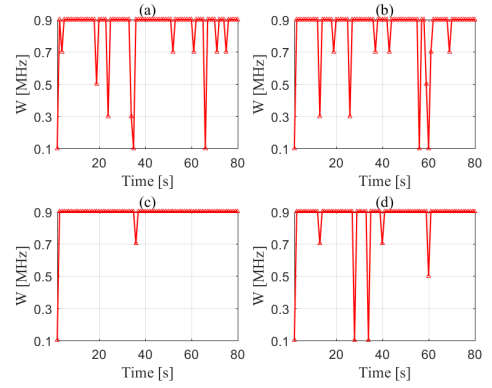


Fig. 17. Waveform bandwidth selection results of the JRO-MDRM scheme in Experiment 2: (a) Airborne radar node 1; (b) Airborne radar node 2; (c) Airborne radar node 3; (d) Airborne radar node 4.

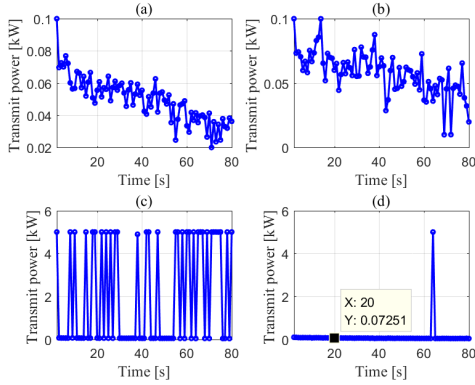


Fig. 15. Transmit power optimization results of the JRO-MDRM scheme in Experiment 2: (a) Airborne radar node 1; (b) Airborne radar node 2; (c) Airborne radar node 3; (d) Airborne radar node 4.

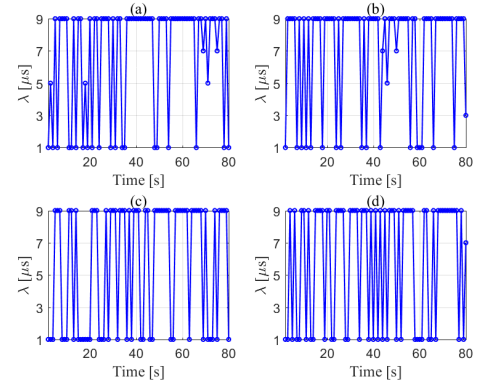


Fig. 18. Waveform pulse length selection results of the JRO-MDRM scheme in Experiment 2: (a) Airborne radar node 1; (b) Airborne radar node 2; (c) Airborne radar node 3; (d) Airborne radar node 4.

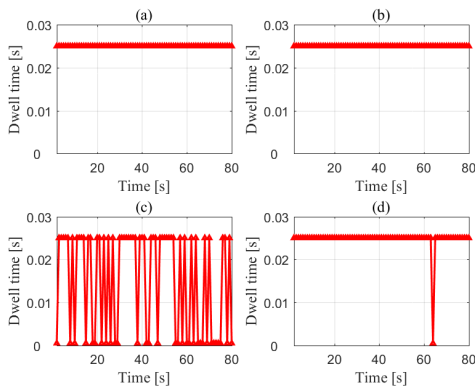


Fig. 16. Dwell time optimization results of the JRO-MDRM scheme in Experiment 2: (a) Airborne radar node 1; (b) Airborne radar node 2; (c) Airborne radar node 3; (d) Airborne radar node 4.

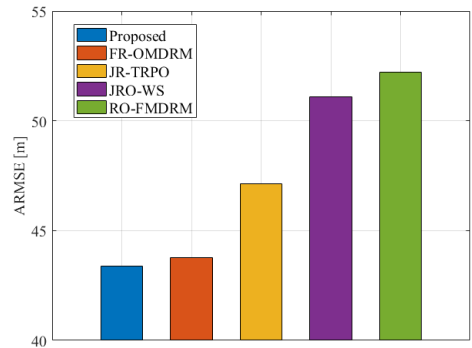


Fig. 19. Target tracking performance comparison in terms of the ARMSE by exploiting various approaches in Experiment 2.

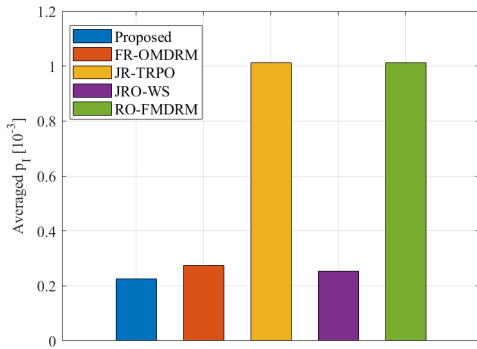


Fig. 20. LPI performance comparison in terms of the averaged probability of intercept by exploiting various approaches in Experiment 2.

radar network by cooperatively optimizing the flight route, illumination power, dwell time, waveform bandwidth, and pulse length of each node, while meeting the kinematic limitations and certain system resource constraints. The joint design is established as a non-linear and non-convex optimization problem. Since the several adaptable variables are coupled in both criterion functions, it is difficult to handle. Subsequently, an iterative algorithm based on PSO and cyclic minimization techniques is developed to achieve the suboptimal solutions with a much lower computational complexity. Numerical results are illustrated to demonstrate that our proposed scheme outperforms the other baseline algorithms. Future research will extend the JRO-MDRM strategy to much more practical scenarios, such as, multi-target tracking scenario, cluttered background, and so forth, and validate the correctness of the developed scheme with real data.

REFERENCES

- [1] R. R. Pitre, X. R. Li, and R. Delbalzo. "UAV route planning for joint search and track missions-An information-value approach," IEEE Transactions on Aerospace and Electronic Systems, 2012, 48(3): 2551-2565.
- [2] X. J. Lu, L. J. Kong, J. Sun, and Y. Yuan. "Joint online route planning and power allocation for multitarget tracking in airborne radar systems," 2020 IEEE Radar Conference (RadarConf20), 2020, 1-6.
- [3] C. G. Shi, L. T. Ding, F. Wang, and S. Salous, J. J. Zhou. "Joint target assignment and resource optimization framework for multitarget tracking in phased array radar network," IEEE Systems Journal, 2020, DOI: 10.1109/JSYST.2020.3025867.
- [4] K. Zhou, and S. I. Roumeliotis. "Optimal motion strategies for range-only constrained multisensor target tracking," IEEE Transactions on Robotics, 2008, 24(5): 1168-1185.
- [5] R. Tharmarasa, T. Kirubarajan, and T. Lang. "Joint path planning and sensor subset selection for multistatic sensor networks," Proceedings of the 2009 IEEE Symposium on Computational Intelligence in Security and Defense Applications (CISDA), 2009, 1-8.
- [6] A. Ghaffarkhah, and Y. Mostofi. "Path planning for networked robotic surveillance," IEEE Transactions on Signal Processing, 2012, 60(7): 3560-3575.
- [7] K. Dogancay. "UAV path planning for passive emitter localization," IEEE Transactions on Aerospace and Electronic Systems, 2012, 48(2): 1150-1166.
- [8] S. Ragi, and E. K. P. Chong. "UAV path planning in a dynamic environment via partially observable Markov decision process," IEEE Transactions on Aerospace and Electronic Systems, 2013, 49(4): 2397-2412.
- [9] N. H. Nguyen, K. Dogancay, and L. M. Davis. "Joint transmitter waveform and receiver path optimization for target tracking by multistatic radar system," IEEE Workshop on Statistical Signal Processing (SSP), 2014, 444-447.
- [10] P. Chen, L. Zheng, X. D. Wang, H. B. Li, and L. N. Wu. "Moving target detection using colocated MIMO radar on multiple distributed moving platforms," IEEE Transactions on Signal Processing, 2017, 65(17): 4670-4683.
- [11] H. V. Nguyen, H. Rezatofighi, B. Vo, and D. C. Ranasinghe. "Online UAV path planning for joint detection and tracking of multiple radio-tagged objects," IEEE Transactions on Signal Processing, 2019, 67(20): 5365-5379.
- [12] Y. Y. Tang, and Y. Wang. "Mobile sensors path planning for cooperative monitoring of different mission importance areas," 2020 IEEE Radar Conference (RadarConf20), 2020, 1-6.
- [13] M. K. Nitalapati, A. S. Bedi, K. Rajawat, and M. Coupechoux. "Online trajectory optimization using inexact gradient feedback for time-varying environments," IEEE Transactions on Signal Processing, 2020, 68: 4824-4838.
- [14] Y. Wu, K. H. Low, and C. Lv. "Cooperative path planning for heterogeneous unmanned vehicles in a search-and-track mission aiming at an underwater target," IEEE Transactions on Vehicular Technology, 2020, 69(6): 6782-6787.
- [15] D. E. Lawrence. "Low probability of intercept antenna array beamforming," IEEE Transactions on Antennas and Propagation, 2010, 58(9): 2858-2865.
- [16] C. W. Zhou, Y. J. Gu, S. B. He, Z. G. Shi. "A robust and efficient algorithm for coprime array adaptive beamforming," IEEE Transactions on Vehicular Technology, 2018, 67(2): 1099-1112.
- [17] M. A. Govoni, H. B. Li, and J. A. Kosinski. "Low probability of intercept of an advanced noise radar waveform with linear-FM," IEEE Transactions on Aerospace and Electronic Systems, 2013, 49(2): 1351-1356.
- [18] C. G. Shi, F. Wang, M. Sellathurai, J. J. Zhou, and S. Salous. "Low probability of intercept-based optimal power allocation scheme for an integrated multistatic radar and communication system," IEEE Systems Journal, 2020, 14(1): 983-994.
- [19] C. G. Shi, F. Wang, S. Salous and J. J. Zhou. "Joint transmitter selection and resource management strategy based on low probability of intercept optimization for distributed radar networks," Radio Science, 2018, 53(9): 1108-1134.
- [20] W. Yi, Y. Yuan, R. Hoseinnezhad, and L. J. Kong. "Resource scheduling for distributed multi-target tracking in netted colocated MIMO radar systems," IEEE Transactions on Signal Processing, 2020, 68: 1602-1617.
- [21] H. W. Zhang, W. J. Liu, Z. J. Zhang, W. L. Lu, and J. W. Xie. "Joint target assignment and power allocation in multiple distributed MIMO radar networks," IEEE Systems Journal, 2020, 15(1): 694-704.
- [22] H. W. Zhang, W. J. Liu, B. F. Zong, and J. P. Shi. "An efficient power allocation strategy for maneuvering target tracking in cognitive MIMO radar," IEEE Transactions on Signal Processing, 2021, 69: 1591-1602.
- [23] J. K. Yan, J. H. Dai, W. Q. Pu, H. W. Liu, and M. Greco. "Target capacity based resource optimization for multiple target tracking in radar network," IEEE Transactions on Signal Processing, 2021, 69: 2410-2421.
- [24] X. Li, T. Cheng, Y. Su, and H. Peng. "Joint time-space resource allocation and waveform selection for the colocated MIMO radar in multiple targets tracking," Signal Processing, 2020, 176: 1-10.
- [25] Y. Su, T. Cheng, Z. S. He, and X. Li. "Joint waveform selection and time-space resource management in netted colocated MIMO radar system for multi-target tracking," 2020 IEEE Radar Conference (RadarConf20), 2020, 1-6.
- [26] M. C. Xie, W. Yi, T. Kirubarajan, and L. J. Kong. "Joint node selection and power allocation strategy for multitarget tracking in decentralized radar networks," IEEE Transactions on Signal Processing, 2018, 66(3): 729-743.
- [27] N. H. Nguyen, K. Dogancay, and L. M. Davis. "Adaptive waveform selection for multistatic target tracking," IEEE Transactions on Aerospace and Electronic Systems, 2015, 51(1): 688-701.
- [28] Y. Yuan, W. Yi, R. Hoseinnezhad, and P. K. Varshney. "Robust power allocation for resource-aware multi-target tracking with colocated MIMO radars," IEEE Transactions on Signal Processing, 2021, 69: 443-458.
- [29] S. P. Boyd, and L. Vandenberghe. "Convex optimization," Cambridge University Press, 2004.
- [30] Y. X. Cai, Z. Q. Wei, R. D. Li, D. W. K. Ng, and J. H. Yuan. "Joint trajectory and resource allocation design for energy-efficient secure UAV communication systems," IEEE Transactions on Communications, 2020, 68(7): 4536-4553.